Characteristics and sources of water-soluble organic aerosol in a heavily polluted environment in Northern China

Li, Haiyan

2021-03-01

Li , H , Zhang , Q , Jiang , W , Collier , S , Sun , Y , Zhang , Q & He , K 2021 , ' Characteristics and sources of water-soluble organic aerosol in a heavily polluted environment in Northern China ' , The Science of the Total Environment , vol. 758 , 143970 . https://doi.org/10.1016/j

http://hdl.handle.net/10138/351861
https://doi.org/10.1016/j.scitotenv.2020.143970

Characteristics and sources of water-soluble organic aerosol in a heavily polluted environment in Northern China

Haiyan Li[1,2,a], Qi Zhang[2,*], Wenqing Jiang[2], Sonya Collier[2], Yele Sun[3,4], Qiang Zhang[5], Kebin He[1]

[1] State Key Joint Laboratory of Environment Simulation and Pollution Control, School of Environment, Tsinghua University, Beijing 100084, China

[2] Department of Environmental Toxicology, University of California, Davis, CA 95616, USA

[3] State Key Laboratory of Atmospheric Boundary Layer Physics and Atmospheric Chemistry, Institute of Atmospheric Physics, Chinese Academy of Sciences, Beijing 100029, China

[4] College of Earth and Planetary Sciences, University of Chinese Academy of Sciences, Beijing 100049, China

[5] Ministry of Education Key Laboratory for Earth System Modeling, Department of Earth System Science, Tsinghua University, Beijing 100084, China

[a] present address: Institute for Atmospheric and Earth System Research/Physics, Faculty of Science, University of Helsinki, 00014 Helsinki, Finland

*Corresponding author

Email address: dkwzhang@ucdavis.edu

Abstract

Water-soluble organic aerosol (WSOA) in fine particles ($PM_{2.5}$) collected during wintertime in a polluted city (Handan) in Northern China was characterized using a High-Resolution Time-of-Flight Aerosol Mass Spectrometer (AMS). Through comparing with real-time measurements from a collocated Aerosol Chemical Speciation Monitor (ACSM), we determined that WSOA on average accounts for 29% of total organic aerosol (OA) mass and correlates tightly with secondary organic aerosol (SOA; Pearson's r = 0.95). The mass spectra of WSOA closely resemble those of ambient SOA, but also show obvious influences from coal combustion and biomass burning. Positive matrix factorization (PMF) analysis of the WSOA mass spectra resolved a water-soluble coal combustion OA (WS-CCOA; O/C=0.17), a water-soluble biomass burning OA (WS-BBOA; O/C=0.32), and a water-soluble oxygenated OA (WS-OOA; O/C=0.89), which account for 10.3%, 29.3% and 60.4% of the total WSOA mass, respectively. The water-solubility of the OA factors was estimated by comparing the offline AMS analysis results with the ambient ACSM measurements. OOA has the highest water-solubility of 49%, consistent with increased hygroscopicity of oxidized organics induced by atmospheric aging processes. In contrast, CCOA is the least water soluble, containing 17% WS-CCOA. The distinct characteristics of WSOA from different sources extend our knowledge of the complex aerosol chemistry in the polluted atmosphere of Northern China and the water-solubility analysis may help us to understand better aerosol hygroscopicity and its effects on radiative forcing in this region.

Keywords: WSOA; polluted environment; source apportionment; aerosol mass spectrometry (AMS); Aerosol Chemical Speciation Monitor (ACSM)

1. Introduction

Water-soluble organic aerosol (WSOA) constitutes 20-80% of organic aerosol (OA) in the atmosphere, depending on the location and season (e.g. Zappoli et al., 1999; Decesari et al., 2000; Decesari et al., 2001; Sullivan et al., 2004; Mader et al., 2004; Huang et al., 2006; Kondo et al., 2007; Sun et al., 2011; Zhang et al., 2012; Du et al., 2014). WSOA can significantly alter the hygroscopicity of atmospheric particles and their ability to act as cloud condensation nuclei (CCN; Saxena et al., 1995; Chan et al., 2008). Therefore, WSOA plays an important role in both direct and indirect effects on radiative forcing. In addition, WSOA can act as surface active reagents, which increase the solubility of hydrophobic organic compounds, such as n-alkanes and polycyclic aromatic hydrocarbons (PAHs), in aqueous phase, and thus increase their toxicity to human health (Wang et al., 2003). The sources of WSOA can be both primary emissions and secondary formation processes. In the absence of biomass burning, WSOA is usually considered a proxy for secondary organic aerosol (SOA) because oxidation reactions tend to impart polar functional groups (e.g. hydroxyl, carbonyl, and carboxyl) to the SOA compounds (Huang et al., 2006; Kondo et al., 2007).

Since WSOA may be composed of numerous polar compounds with a wide range of physical chemical properties (Saxena and Hildemann, 1996), it is challenging to characterize the composition and sources of WSOA. Typically, the individually identified compounds explain less than 20% of total WSOA mass (Graham et al., 2002; Zhang et al., 2002). However, by combining a Particle-Into-Liquid-Sampler (PILS) with a total carbon (TOC) analyzer, Sullivan et al. (2004) was able to quantify the water-soluble organic carbon content in ambient particles. In recent years, the Aerodyne Aerosol Mass Spectrometer (AMS) has been widely used for characterizing bulk composition of OA in both ambient and laboratory studies. The quantitative and highly time-

resolved AMS measurement data facilitate source apportionment of ambient OA via factor analysis (Zhang et al., 2011). Oxygenated OA (OOA) was a commonly identified OA factor and it was found to be primarily composed of water-soluble species (Kondo et al., 2007). In addition, AMS has been applied successfully to characterize WSOA in aqueous samples. For example, recent studies have demonstrated the utility of AMS for elucidating the chemical composition and formation mechanisms of WSOA formed from aqueous-phase reactions of phenolic volatile organic compounds (VOCs) (Sun et al., 2010; Yu et al., 2014; Yu et al., 2016). Sun et al. (2011) performed the first AMS analysis of water extracts of atmospheric fine particles ($PM_{2.5}$) and investigated the sources of WSOA in southeastern U.S. via PMF analysis of the WSOA AMS mass spectra. The source apportionment results of WSOA can be combined with collocated AMS measurements of ambient OA to estimate the water-solubility of different OA factors. For instance, Xu et al. (2017) investigated the water-solubility of hydrocarbon-like OA (HOA), cooking OA (COA), and three types of SOA factors through online collection and quantification of both WSOA and total ambient OA by coupling a PILS with a High-Resolution Time-of-Flight AMS. Qiu et al. (2019) explored the vertical differences in the chemical characteristics and water-solubility of different OA factors in Beijing, China, by performing offline AMS analysis of the water extracts of PM filters collected simultaneously during online AMS measurements. Since the water-solubility of OA affects the chemical and microphysical properties of aerosols, such as their acidity, optical properties, and CCN activities (Jacobson et al., 2000), it is important to improve our understanding of the water-solubility of OA factors representing different emission sources and atmospheric chemical processes.

With rapid industrialization and urbanization, air pollution in Northern China has become a severe problem and has raised global concerns in recent years. Along with the water-soluble

characteristics, WSOA at high particulate matter (PM) loadings seriously threatens air quality, regional and global climates, and human health. However, limited information is available on the chemical properties and sources of WSOA in Northern China, despite the fact that WSOA was found to account for approximately 50% of total OA in this region (Pathak et al., 2011; Du et al., 2014). Zong et al. (2016) investigated the diurnal characteristics of WSOA in the Yellow River Delta and found that biomass burning and fossil fuel combustion may largely contribute to WSOA based on the correlation analysis with tracer species. Luo et al. (2020) showed that high aerosol liquid water and particle acidity enhanced the formation of WSOA at a background site of Northern China. Here, we utilized a High-Resolution Time-of-Flight AMS (AMS hereafter) to analyze WSOA in $PM_{2.5}$ collected in wintertime in Handan, China. According to the 2018 World Air Quality Report, Handan is one of the top 10 polluted cities in China, where air pollution arises from contributions from various types of emission sources and thus highly complex atmospheric chemistry. We performed PMF analysis to the high-resolution mass spectra (HRMS) of WSOA to resolve various sources that exhibit distinguishing chemical characteristics. In addition, an ACSM was deployed to provide real-time measurements of ambient OA composition during the same sampling period. The water-solubility of different OA factors was subsequently determined by comparing their water-soluble portions to ambient concentrations.

2. Experimental methods

2.1 Aerosol sampling

Both filter sampling and real-time measurements were conducted at Hebei University of Engineering (36.57°N, 114.50°E) in Handan, China. Handan is located in the crossing area of four provinces, bordering Xingtai of Hebei province to the north, Shanxi province to the west, Henan province to the south and Shandong province to the east, all of which are heavily populated,

industrialized and urbanized. Handan itself is well known for heavy industrial outputs of steel, iron and cement, which result in high local emissions of air pollutants. Our sampling site is situated on the southeast edge of urban Handan, on the roof of a four-story building (~12 m above the ground) inside the university campus, The site is surrounded by residential areas and is located ~300 m north of the South Ring Road and ~400 m northeast of Handan Highway (S313). In this work, a total of 44 $PM_{2.5}$ samples (12-h integrated) were collected on pre-baked (500^{o}C) quartz filters using a high-volume sampler (Thermo Scientific, MA, USA) from December 10, 2015 to December 31, 2015. The daytime samples were collected from 08:00 to 19:30 (local time = UTC+8), and the nighttime samples were collected from 20:00 to 07:30 of the next day. Field blanks were collected using the same method as for the exposed filters. An ACSM was deployed at the same site from December 3, 2015 to February 5, 2016 to measure the mass concentrations of non-refractory submicron aerosol (NR-PM_1) species, including organics, sulfate, nitrate, ammonium and chloride, in real-time. Details on the ambient ACSM measurements and data analysis can be found in Li et al. (2017).

2.2 Offline AMS analysis and determination of water-soluble components

For each filter sample, one square piece (6.45 cm^2) was collected and sonicated in 15 mL Milli-Q water at ~ 0^{o}C for 45 min. The solution was then filtered with 0.45 μm PTFE syringe filters. The aerosol extractions were aerosolized by pure nitrogen using a constant output atomizer and dehumidified via a diffusion dryer. The resulting particles were subsequently sampled into the AMS and analyzed under both the high sensitive V-mode and the high mass resolution W-mode (mass resolution m/Δm ~6000). Between every two samples, a Milli-Q water sample was nebulized and analyzed in the same way to reduce carry-over effects and serve as an analytical

129 blank. The field blank samples were analyzed using the same procedures as the filter samples.
130 Details on AMS analysis of liquid samples are given in Sun et al (2010) and Sun et al. (2011).

131 The AMS data were processed using standard AMS data analysis software SQUIRREL v1.56
132 and PIKA v1.15 written in Igor Pro (Wavemetrics, Lake Oswego, OR). Default relative ionization
133 efficiency (RIE) values were assumed for organics (1.4), nitrate (1.1), and chloride (1.3), while an
134 RIE value of 4.54 was determined for ammonium and 1.05 for sulfate following the analysis of
135 pure NH_4NO_3 and $(NH_4)_2SO_4$, respectively. Previous study found that ammonium nitrate can cause
136 interference on CO_2^+ signal in the AMS mass spectra (Pieber et al., 2016). The magnitude of this
137 artifact was found to be highly dependent on instruments and aerosol chemical composition (Pieber
138 et al., 2016; Freney et al., 2019). According to analysis of pure ammonium nitrate and ammonium
139 sulfate particles, their impacts on organic CO_2^+ signal was found to be negligible with our
140 instrument, ~0.9% from ammonium nitrate and ~0.4% from ammonium sulfate. Therefore, a
141 correction was not applied for the quantification of CO_2^+ signal. With nitrogen as the carrier gas,
142 it is challenging to accurately determine the CO^+ signal produced from oxygenated species due to
143 the interference of the very large N_2^+ signal at *m/z* 28. Thus, the CO^+ signal was scaled to the
144 measured CO_2^+ signal using the CO^+/CO_2^+ ratio determined for the WSOA when argon was used
145 as the carrier gas. Elemental analysis was performed on the ion-speciated high-resolution mass
146 spectra (HRMS) up to *m/z* 120 to determine the atomic oxygen-to-carbon (O/C), hydrogen-to-
147 carbon (H/C), nitrogen-to-carbon (N/C), and organic mass-to-carbon (OM/OC) ratios following
148 the Improved-Ambient (IA) method (Canagaratna et al., 2015). The elemental ratios were also
149 calculated using the previously published Aiken-Ambient (AA) method (Aiken et al., 2008) to
150 compare with literature results.

In order to relate the species concentration in the nebulized aerosol to that in ambient air, the sulfate signal was used as an internal standard. Basically, since sulfate is nonvolatile and water-soluble, we assume it was extracted at 100% efficiency by water. Thus, the concentration of organic matter measured by the AMS in the nebulized aerosol ($[Org]_{AMS}$) can be converted to ambient concentration (WSOA) by applying the ratio between the sulfate concentration measured in filter extract by the AMS ($[SO_4^{2-}]_{AMS}$) and the average ambient sulfate concentration measured by ACSM over the corresponding time period ($[SO_4^{2-}]_{ACSM}$):

$$WSOA = [Org]_{AMS} \times \frac{[SO_4{}^{2-}]_{ACSM}}{[SO_4{}^{2-}]_{AMS}} \quad \text{(Eq.1)}$$

In this way, the scaled WSOA concentration corresponds to the size range of PM_1. The assumption is that ambient sulfate is quantitatively extracted and measured by the AMS. We also assume that the fractional composition in the size range sampled by ACSM and filter samples is the same. The water-soluble fraction of different species is calculated as the ratio of their water-soluble concentration over the average species concentration measured by ACSM.

As shown in Figure S1, the water-soluble fraction of each species is well correlated with their concentration in ambient air. Based on the regression slope, water-soluble matter (WSM) accounts for an average fraction of 54% of total ambient submicron aerosol. It should be noted that ammonium nitrate, ammonium chloride, and a significant fraction of the less oxidized organics are semivolatile species (Karydis et al., 2011). Therefore, their water-solubility can be underestimated due to evaporation during filter sampling (Romakkaniemi et al., 2014). The application of two different instruments in this study, AMS and ACSM, may cause uncertainties as well. While the high-resolution capabilities of AMS allow the direct separation of most ions from inorganic and organic species at the same nominal *m/z*, the quadrupole detector of ACSM

limits the mass resolving power to unity and provides reduced sensitivity, especially for organics (DeCarlo et al., 2006; Timonen et al., 2016). Moreover, the water-solubility of each species calculated in this study may be affected by the fractional composition in different size ranges sampled by the ACSM and the filter sampler.

2.3 Factor analysis of WSOA using ME-2

To investigate the sources of WSOA, PMF was performed on the HRMS of WSOA using the multilinear engine algorithm (ME-2) (Paatero, 1999) implemented with the toolkit SoFi (Source Finder) developed by Canonaco et al. (2013). The so-called *a* value approach allows the user to add a priori information into the model (e.g., known source profiles or time series) to reduce the rotational ambiguity and to separate the mixed or weak solution. The mass spectra and error matrices of organics were prepared according to the protocol summarized by Ulbrich et al. (2009) and Zhang et al. (2011). In this study, because the HRMS of WSOA display obvious characteristics of coal combustion and biomass burning, we constrained coal combustion OA (CCOA) and biomass burning OA (BBOA) (ambient profiles adapted from Sun et al., 2015) and optimized the solution by investigating different combinations of *a* values varying from 0 to 1 (step = 0.1). A thorough evaluation of the solutions was conducted, including comparing the mass spectra of different factors with previously reported reference profiles, comparing the time series of the factors with those of ambient OA factors resolved from PMF analysis of the real-time ACSM data, and investigating residual variations of specific tracer ions and their distribution behaviors among different OA factors. After these procedures, a three-factor solution with the fixed *a* value of 0.6 for CCOA and 0.5 for BBOA was chosen as the optimal solution. Given that the mass spectra of water-soluble OA factors may vary significantly from those of ambient OA factors, the *a* values of 0.6 and 0.5 in this work give the ME-2 model relatively large freedom to vary from the initial

196 constraints. Note that we also performed ME-2 analysis by constraining hydrocarbon-like OA
197 (HOA), in addition to CCOA and BBOA, as an HOA factor associated with vehicle emissions was
198 resolved in the ambient observations in Handan during the sampling period (Li et al., 2017).
199 However, WS-HOA appears to be a negligible fraction of WSOA in this study. For instance, when
200 the *a* value was increased for HOA, the resulting "HOA" mass spectra tended to show strong
201 characteristics of BBOA and their concentrations were low. This result is consistent with the low
202 water-solubility of HOA (Daellenbach et al., 2016; Xu et al., 2017) and its small fraction in
203 ambient PM in Handan (Li et al., 2017). Thus no constraint was applied to HOA in the ME-2
204 analysis. Similarly, HOA was not identified in WSOA in Beijing (Qiu et al., 2019).

205 **3 Results and discussion**

206 **3.1 Characteristics of water-soluble components**

207 An overview of the chemical composition of the water-soluble components and ambient
208 particles is illustrated in Figure 1. While the ambient NR-PM_1 is dominated by organics (47%),
209 the water extract is mainly composed of sulfate and WSOA, with the average contributions of 32%
210 and 27%, respectively. This large difference in the fractional composition indicates the significant
211 contribution of water-insoluble OA in Handan. Therefore, it should be cautious for studies to
212 explore the chemistry of organic aerosol solely based on the water extracts of atmosphere particles,
213 especially in the heavily polluted atmosphere.

214 On average, the water-soluble fraction of OA is around 29% in Handan during wintertime
215 (Figure 2a), much lower than that (~50%) observed in other areas of Northern China (Pathak et al.,
216 2011; Du et al., 2014; Qiu et al., 2019). The low water-solubility of OA in Handan is probably
217 caused by more primary emissions of OA in this region (Li et al. 2017), which are mainly water-

insoluble and will be discussed in Section 3.4. Figure 2b shows that WSOA is tightly correlated with ambient SOA measured by ACSM ($r^2 = 0.9$), which is consistent with previous findings that SOA is mainly water-soluble (Kondo et al., 2007). However, the fact that the regression slope of WSOA vs. SOA is smaller than unity indicates that not all the SOA compounds are water-soluble, for example, SOA compounds with large carbon-hydrogen functional groups tend to have low water-solubility (Saxena and Hildemann, 1996; Robinson et al., 2007).

Both the water-soluble aerosol and ambient aerosol are not bulk neutralized, as shown in Fig. 3 the scatter plot of the observed NH_4^+ concentration vs. the predicted NH_4^+ required to fully neutralize the measured SO_4^{2-}, NO_3^-, and Cl^- (Zhang et al., 2007). It has been found that the fraction of nonvolatile cations (i.e., Na^+, K^+, Ca^{2+}, and Mg^{2+}) in PM_1 in Beijing is generally negligible compared to other species (Sun et al., 2014). The measured/predicted NH_4^+ ratios are ~ 0.75 for both water-soluble and ambient aerosol, indicating that on average ~ 50% of the sulfate molecules in fine particles in Handan are present in the form of NH_4HSO_4. The measured/predicted NH_4^+ ratio in this study can be underestimated due to the presence of organonitrates, organosulfates or organic acids in aerosols. These species would increase the concentrations of the nominally identified inorganic nitrate and sulfate by AMS and ACSM, and thus affect the observed ammonium balance (Farmer et al., 2010).

3.2 Mass spectral features of WSOA

Figure 4 compares the average HRMS of WSOA characterized by the contribution of different ion categories to the average UMR mass spectrum of ambient OA measured by ACSM. While ambient OA shows a much higher relative abundance of MS peaks at larger *m/z*'s, the HRMS of WSOA presents more oxidized characteristics corresponding to SOA. Similarly, the AMS mass spectra of WSOA showed highly oxidized features in southeastern US (Sun et al., 2011)

and eastern China (Ye et al., 2017). In addition, in Zurich, where OA composition was dominated by secondary species, Daellenbach et al. (2016) reported that the mass spectra of WSOA measured by offline AMS are similar to those of ambient OA from online ACSM. In this study the substantial difference between the mass spectra of WSOA and ambient OA is attributed to the large contribution of primary OA in Handan (Li et al., 2017), which is usually much less soluble compared to SOA (Saxena and Hildemann, 1996).

The HRMS of WSOA displays elevated peaks at *m/z* 60 ($C_2H_4O_2^+$), *m/z* 73 ($C_3H_5O_2^+$)—the AMS spectral markers for BBOA (Cubison et al., 2011), and *m/z* 115 ($C_9H_7^+$)—the AMS spectral marker for CCOA (Li et al., 2017; Xu et al., 2020), demonstrating the influence of biomass burning and coal combustion. This is in line with the fact that ambient OA in Handan during wintertime has significant contributions from biomass and coal combustions (Li et al., 2017). Indeed, the UMR spectrum of WSOA shows high peaks at *m/z* > 150 and indicate the abundance of high-molecular-weight species (Fig. S2). We further estimate the concentration of water-soluble PAHs based on the method by Dzepina et al. (2007). The average PAHs concentration in water extracts is 46.3 ng/m^3 in this study, much lower than that observed in the ambient in Northern China due to the low water-solubility of PAHs (Okuda et al., 2006; Liu et al., 2007), but much higher than that measured in U.S. and Europe (Primbs et al., 2008; Ravindra et al., 2008).

As shown in Figure 5, WSOA has an average OM/OC ratio of 1.96 (OM/OC_{AA}, the OM/OC calculated with Aiken-Ambient method, is 1.80), agreeing well with the previously reported values (1.7-2.0) (Sun et al., 2011; Ye et al., 2017; Xu et al., 2017). The average O/C ratio of the WSOA is 0.61 (O/C_{AA} = 0.46), falling in the range of the O/C ratios of SV-OOA (0.35±0.14) and LV-OOA (0.73±0.14) from multiple field studies in the Northern Hemisphere (Ng et al., 2010). The N/C ratios of WSOA vary between 0.04 and 0.08, generally higher than the values of ambient OA

observed in winter in Northern China (Zhang et al., 2014; Hu et al., 2016; Sun et al., 2016; Xu et al., 2016), which could be explained by the hydrophilic properties of nitrogen-containing functional groups (Saxena and Hildemann et al., 1996; Zhang et al., 2002). Accordingly, the HRMS of WSOA have a high fraction of nitrogen-containing ions (13%), e.g. $C_xH_yN^+$ and $C_xH_yNO^+$ (Figure 4c), suggesting the dominance of reduced nitrogen functional groups including amines, amino acids, and amides (Sun et al., 2011). Organonitrate (ON) could also probably exist especially considering the high emissions of both VOCs and NO_x in Northern China. However, ON is fairly water-insoluble according to previous observations (Sullivan et al., 2006; Miyazaki et al., 2009). In addition, due to the extensive fragmentation of ON molecules by electron ionization in the AMS, Farmer et al. (2010) showed that ON standards mostly appear as NO_x^+ ions with minor contribution of nitrogen functional groups. The NO^+/NO_2^+ ratio in the aerosol mass spectrum is substantially higher for ON than ammonium nitrate (Fry et al., 2009, 2013; Bruns et al., 2010). The NO^+/NO_2^+ ratio in this study shows an average value of 2.39, similar to that of pure ammonium nitrate (2.47). Therefore, the contribution of ON to WSOA is negligible in this work. Given that amines and amides can be emitted from biomass burning and various industrial processes (Ge et al., 2011; Yao et al., 2016), the high intensity of combustion and industrial activities in Handan may be important sources of the nitrogen-containing species.

The HRMS of WSOA are also characterized by several sulfur-containing organic ions, especially a distinct peak of $CH_3SO_2^+$ (Figure 4d). $CH_3SO_2^+$ has previously been considered a marker ion for methylsulfonic acid (MSA), which is typically associated with ocean emissions but has been found to have terrestrial sources as well (Ge et al., 2012). Recently, laboratory studies using organosulfate (OS) standard suggested that $CH_3SO_2^+$ is also indicative of OS (Farmer et al., 2010). The existence of OS is further evidenced by the far different signal intensity ratios of

287 $CH_2SO_2^+$, $CH_3SO_2^+$, and $CH_4SO_3^+$ ($CH_2SO_2^+/CH_3SO_2^+$=0.09; $CH_4SO_3^+/CH_3SO_2^+$=0.15) in this
288 study from those observed in the mass spectrum of pure MSA (Ge et al., 2012).

289 **3.3 Source Apportionment of WSOA**

290 Three major sources of WSOA are identified in this study via ME-2 analysis of the HRMS
291 of WSOA, namely water-soluble CCOA (WS-CCOA), water-soluble BBOA (WS-BBOA), and
292 water-soluble OOA (WS-OOA). Figure 6 provides a summary of the mass spectral profiles, time
293 series, and the mass fractional contributions of these factors.

294 As shown in Figure 6a, the mass spectrum of WS-CCOA is dominated by alkyl fragments
295 ($C_nH_{2n+1}^+$ and $C_nH_{2n-1}^+$), typical of POA ions from fossil fuel combustion. Consistent with
296 ambient observations (Hu et al., 2013; Hu et al., 2016; Sun et al., 2016), WS-CCOA presents a
297 unique peak of $C_9H_7^+$ at *m/z* 115, the spectral marker of coal combustion. The O/C and H/C ratios
298 of WS-CCOA are 0.17 and 1.80, respectively. Because the mass spectrum of WS-CCOA in this
299 study is to some extent constrained by the ambient reference profile introduced into ME-2, the
300 deviation of WS-CCOA from the constraint profile could provide some specific insights into the
301 distinguishing features of water-soluble OA from coal combustion. Compared with the CCOA
302 reference profile determined via PMF analysis of ambient AMS mass spectra in Northern China
303 (Sun et al., 2015; Figure S3), the mass spectrum of WS-CCOA is characterized by higher fractions
304 of oxygen-containing ions ($C_xH_yO^+$ and $C_xH_yO_2^+$) at specific *m/z*'s, suggesting that WS-CCOA is
305 more oxidized than ambient CCOA. Correspondingly, the O/C ratio of WS-CCOA is a bit higher
306 than that of ambient CCOA (0.11). In addition, the mass spectrum of WS-CCOA shows
307 significantly lower abundance of signals at larger *m/z*'s compared to ambient CCOA, probably due
308 to the low water solubility of PAHs and long-chain alkanes, which are usually present in high
309 concentration in coal combustion OA (Zhang et al., 2008). The average mass concentration of WS-

CCOA is 3.3 μg m^{-3}, accounting for 10.3% of total WSOA (Figure 6h). The time series of WS-CCOA is poorly correlated with those of ambient CCOA (r^2=0.21; Figure 7a), which could be caused by the high variability in the water-soluble fraction of CCOA under different conditions. Poor correlations between the water-soluble portion and ambient fraction of OA factors have also been observed for HOA and COA in southeastern US (Xu et al., 2017).

WS-BBOA on average accounts for 29.3% of WSOA, in accordance with the significant contribution of BBOA in ambient conditions in Handan due to domestic combustion of wood and crop residuals for cooking and home heating (Li et al., 2017). Previous studies have indicated that biomass burning is an important source of WSOA since primary BBOA are composed of moderately water-soluble species such as anhydrous sugar and biomass burning emissions may undergo substantial chemical aging directly after emitted and during atmospheric transport, forming oxidized BBOA (Cubison et al., 2011; Zhou et al., 2017). The mass spectrum of WS-BBOA is dominated by $C_xH_y^+$ (46%) and $C_xH_yO_z^+$ (41%) ions. Consistent with ambient measurements, WS-BBOA is characterized by prominent peaks at *m/z* 60 and *m/z* 73, dominated by $C_2H_4O_2^+$ and $C_3H_5O_2^+$, respectively, both of which are typical ion fragments of anhydrous sugars (e.g., levoglucosan) (Cubison et al., 2011). Another remarkable MS feature of WS-BBOA is the higher mass fraction of $C_xH_yN_q^+$ ions (11%), and a moderately high average N/C ratio of 0.05. The enrichment of nitrogen-containing organic compounds in BBOA has also been observed in previous studies (Lobert et al., 1990; Laskin et al., 2009). The temporal variations of WS-BBOA are closely correlated with those of ambient BBOA (r^2 = 0.91; Figure 6e; Figure 7b), similar to the findings from a previous study at a rural site in the southeastern US (Xu et al., 2017).

SOA has traditionally been accepted as the major contributor to WSOA in $PM_{2.5}$. In this study, the mass spectrum of WS-OOA is quite similar to that of ambient OOA, characterized by a

prominent peak of *m/z* 44 (mainly CO_2^+). WS-OOA has a high O/C ratio of 0.89, falling in the range of the O/C ratios of ambient LV-OOA observed across multiple sites in the Northern Hemisphere (Ng et al., 2010). On average, WS-OOA accounts for 60.4% of total WSOA with an average concentration of 19.1 μg m^{-3}. Consistent with the observations of Daellenbach et al. (2016) and Xu et al. (2017), the time series of WS-OOA strongly correlates with those of ambient OOA (r^2=0.98; Figure 7c).

Different from ambient measurements in Handan (Li et al., 2017), no water-soluble OA factor associated with traffic emissions was resolved, indicating that the water-soluble fraction of HOA is negligible in this work. Xu et al. (2017) also showed that the resolved HOA in the southeastern US was largely water-insoluble. According to Sun et al. (2012), a large fraction of OA is contributed by OOA at a site right next to a busy highway.

The WSOA concentration was also reconstructed by a multivariate linear regression model with the ambient observed HOA, CCOA, BBOA, and OOA factors. As displayed in Figure S4, the predicted WSOA correlates very well with the measured WSOA (r^2=0.98; predicted WSOA=0.51×OOA+0.35×BBOA+2.80). On average, the reconstructed WSOA is composed of 58% OOA and 29% BBOA, concurring with the results of the ME-2 source apportionment.

3.4 Water-solubility of OA factors

By comparing the water-soluble portion to ambient fraction, we calculate the water-solubility of various OA factors. Some data points greater than 1 are observed when the concentration of water-soluble OA factors is higher than that of ambient OA factors. This may be caused by uncertainties associated with ME-2 analysis and inconsistency between the two instruments. As

the mean value may be biased by outlier points in the time series of $[C]_{water\text{-}soluble}/[C]_{ambient}$ ratio, we use the median value to evaluate the water-solubility of different OA factors.

CCOA has the lowest water-solubility of 16.5% (3.5% to 36.0% for 10^{th} and 90^{th} percentiles) among all resolved OA factors in this study (Figure 8). This is consistent with the fact that PAHs and n-alkanes are the dominant species from residential coal combustion (Zhang et al., 2008), which are largely water-insoluble (May et al., 1978; Capel et al., 1991). The water-solubility of CCOA in this study is much lower than that observed in Beijing during wintertime (Qiu et al., 2019), likely due to the fact that CCOA is generally much less oxidized and is more related to the direct local emissions in the heavily polluted atmosphere in Handan.

Regarding to BBOA, about 37.2% (24.7% to 59.8% for 10^{th} and 90^{th} percentiles) of its mass is water-soluble in Handan. The water-solubility of BBOA in this study is much lower than those observed by Daellenbach et al. (2016), Xu et al. (2017), and Qiu et al. (2019) using similar methods (Figure 8). Indeed, a sizable range of the water-solubility of BBOA has been previously reported. For instance, by collecting BBOA samples from burning pine needles and sticks, Bateman et al. (2010) observed significant difference in BBOA mass spectra between water and acetonitrile extractions, demonstrating that BBOA is dominated by a water-insoluble fraction (estimated WSOC fraction ~40%). On the other hand, using a multilinear regression analysis, Sciare et al. (2011) estimated that 82% of OC in wood burning is water-soluble. The large variation in BBOA water-solubility is likely caused by differences in fuel types, burning conditions, and atmospheric aging processes (Heringa et al., 2011). Consistently, three types of BBOA factors have been identified in the wildfire plumes (Zhou et al., 2017).

Among all OA factors, OOA has the highest water-solubility of 48.6% (36.6% to 56.3% for 10^{th} and 90^{th} percentiles). This is in accordance with the fact that OOA represents OA that has

undergone aging processes in the atmosphere. Previous studies have shown that OA becomes more oxidized, more hygroscopic, and thus more water-soluble during aging (Robinson et al., 2007; Jimenez et al., 2009). Kondo et al. (2007) first examined the relationship between OOA and WSOC and found that they have very similar chemical characteristics. The water-solubility of OOA in Handan is much lower than that reported in Switzerland (Daellenbach et al., 2016) but similar to that observed in Beijing (Qiu et al., 2019), suggesting that OOA in Northern China is less aged, and is probably the product of intermediately aged primary anthropogenic emissions. Accordingly, the water-solubility of OOA in this work is similar to that of less-oxidized oxygenated OA (LO-OOA) observed by Xu et al. (2017) (Figure 8).

4. Implications and conclusions

Extensive studies in China have revealed that OA is a dominant component in PM and that a thorough understanding of ambient OA chemistry is crucial for addressing the widespread air pollution problem in the country (Li et al., 2017; Zhou et al., 2020 and references therein). AMS and ACSM are the most powerful instruments utilized worldwide for characterizing atmospheric aerosol chemical composition in real-time (Parworth et al., 2015; Li et al., 2019; Heikkinen et al., 2020). However, given the limited availability of these instruments compared to filter samplers, a methodology of using offline AMS to characterize OA based on the water extracts of filter samples has been developed and applied in several recent studies (Huang et al., 2014; Daellenbach et al., 2016, 2017; Bozzetti et al., 2017a, 2017b; Ye et al., 2017). According to our results, WSOA only accounts for approximately 29% of total OA, indicating a relatively low water-soluble fraction of OA in the polluted Northern China region. Therefore, it is difficult to get a comprehensive view of OA characteristics only through analyzing the water extracts of particles in Northern China, especially during wintertime when intensive primary emissions release largely water-insoluble

primary OA species. Moreover, the mass spectra of WSOA and total OA indicate large differences in their chemical characteristics. These results emphasize a major limitation with offline AMS analysis of PM filter samples in polluted environments and potential biases of extrapolating the findings on WSOA to interpret total OA behaviors during wintertime in Northern China.

Despite the fact that CCOA is mostly composed of hydrophobic components, the water-soluble fraction of CCOA may contain various PAHs. Psichoudaki et al. (2013) showed that some PAHs (i.e., fluoranthene, benzoanthracene and benzoperylene) can be extracted by water to high efficiency, even close to 100%. These water-soluble PAHs pose a threat to human health. It is well known that coal combustion is not an important source of air pollution in the US or Europe due to stricter emission controls. However, combustion of coals is found to be a large emitter of organic air pollutants in China (Cao et al., 2006; Zhang et al., 2008), especially during wintertime when coal is primarily used for residential and commercial heating in Northern China. Therefore, the potential health effects of the water-soluble fraction of CCOA should be seriously considered.

Overall, this study presents the characterization of WSOA in a heavily polluted city in Northern China. Due to the high emissions of OA from primary combustion sources, WSOA accounts for a much lower fraction of the total OA mass in Handan than in other areas. Via source apportionment analysis of WSOA and comparison with collocated ambient OA measurements, the water-solubility of OA from coal combustion, biomass burning, and secondary formation processes is estimated and found to be highly variable. OA from vehicle emissions appears to be mostly water insoluble. These results indicate that the bulk hygroscopic property of ambient OA in Northern China likely demonstrates significant variabilities that are dependent on the location and time.

Credit authorship contribution statement

Haiyan Li: Conceptualization, Methodology, Formal analysis, Writing - original draft. **Qi Zhang**: Conceptualization, Methodology, Supervision, Writing - review & editing. **Wenqing Jiang**: Methodology, Investigation. **Sonya Collier**: Methodology, Writing - review & editing. **Yele Sun**: Writing - review & editing. **Qiang Zhang**: Resources, Supervision, Writing - review & editing. **Kebin He**: Supervision, Writing - review & editing.

Declaration of competing interest

The authors declare that they have no known competing financial interests or personal relationships that could have appeared to influence the work reported in this paper.

Acknowledgements

This work was funded by the National Natural Science Foundation of China (41571130035 and 41625020). We give special acknowledgement to lab members in the Department of Environmental Engineering, Hebei University of Engineering, Handan, China, who helped us with the collection of filter samples.

References

Aiken, A. C., Decarlo, P. F., Kroll, J. H., Worsnop, D. R., Huffman, J. A., Docherty, K. S., Ulbrich, I. M., Mohr, C., Kimmel, J. R., Sueper, D., Sun, Y., Zhang, Q., Trimborn, A., Northway, M., Ziemann, P. J., Canagaratna, M. R., Onasch, T. B., Alfarra, M. R., Prevot, A. S. H., Dommen, J., Duplissy, J., Metzger, A., Baltensperger, U., and Jimenez, J. L.: O/C and OM/OC ratios of primary, secondary, and ambient organic aerosols with high-resolution time-of-flight aerosol mass spectrometry, Environ Sci Technol, 42, 4478-4485, 10.1021/es703009q, 2008.

Bateman, A. P., Nizkorodov, S. A., Laskin, J., and Laskin, A.: High-Resolution Electrospray Ionization Mass Spectrometry Analysis of Water-Soluble Organic Aerosols Collected with a Particle into Liquid Sampler, Anal Chem, 82, 8010-8016, 10.1021/ac1014386, 2010.

Bozzetti, C., Sosedova, Y., Xiao, M., Daellenbach, K. R., Ulevicius, V., Dudoitis, V., Mordas, G., Byčenkienė, S., Plauškaitė, K., Vlachou, A., Golly, B., Chazeau, B., Besombes, J. L., Baltensperger, U., Jaffrezo, J. L., Slowik, J. G., El Haddad, I., and Prévôt, A. S. H.: Argon offline-AMS source apportionment of organic aerosol over yearly cycles for an urban, rural, and marine site in northern Europe, Atmos. Chem. Phys., 17, 117-141, 10.5194/acp-17-117-2017, 2017a.

Bozzetti, C., El Haddad, I., Salameh, D., Daellenbach, K. R., Fermo, P., Gonzalez, R., Minguillón, M. C., Iinuma, Y., Poulain, L., Müller, E., Slowik, J. G., Jaffrezo, J. L., Baltensperger, U., Marchand, N., and Prévôt, A. S. H.: Organic aerosol source apportionment by offline-AMS over a full year in Marseille, Atmos. Chem. Phys. Discuss., 2017, 1-46, 10.5194/acp-2017-54, 2017b.

Bruns, E. A., Perraud, V., Zelenyuk, A., Ezell, M. J., Johnson, S. N., Yu, Y., Imre, D., Finlayson-Pitts, B. J., and Alexander, M. L.: Comparison of FTIR and Particle Mass Spectrometry for the Measurement of Particulate Organic Nitrates, Environ Sci Technol, 44, 1056-1061, 10.1021/es9029864, 2010.

Canonaco, F., Crippa, M., Slowik, J. G., Baltensperger, U., and Prevot, A. S. H.: SoFi, an IGOR-based interface for the efficient use of the generalized multilinear engine (ME-2) for the source apportionment: ME-2 application to aerosol mass spectrometer data, Atmos Meas Tech, 6, 3649-3661, 10.5194/amt-6-3649-2013, 2013.

Cao, G. L., Zhang, X. Y., and Zheng, F. C.: Inventory of black carbon and organic carbon emissions from China, Atmos Environ, 40, 6516-6527, 10.1016/j.atmosenv.2006.05.070, 2006.

Capel, P. D., Leuenberger, C., and Giger, W.: Hydrophobic organic chemicals in urban fog, Atmospheric Environment. Part A. General Topics, 25, 1335-1346, https://doi.org/10.1016/0960-1686(91)90244-2, 1991.

Chan, M. N., Kreidenweis, S. M., and Chan, C. K.: Measurements of the hygroscopic and deliquescence properties of organic compounds of different solubilities in water and their relationship with cloud condensation nuclei activities, Environ Sci Technol, 42, 3602-3608, 10.1021/es7023252, 2008.

Cubison, M. J., Ortega, A. M., Hayes, P. L., Farmer, D. K., Day, D., Lechner, M. J., Brune, W. H., Apel, E., Diskin, G. S., Fisher, J. A., Fuelberg, H. E., Hecobian, A., Knapp, D. J., Mikoviny, T., Riemer, D., Sachse, G. W., Sessions, W., Weber, R. J., Weinheimer, A. J., Wisthaler, A., and Jimenez, J. L.: Effects of aging on organic aerosol from open biomass burning smoke in aircraft and laboratory studies, Atmos Chem Phys, 11, 12049-12064, 10.5194/acp-11-12049-2011, 2011.

DeCarlo, P. F., Kimmel, J. R., Trimborn, A., Northway, M. J., Jayne, J. T., Aiken, A. C., Gonin, M., Fuhrer, K., Horvath, T., Docherty, K. S., Worsnop, D. R., and Jimenez, J. L.: Field-deployable, high-resolution, time-of-flight aerosol mass spectrometer, Anal Chem, 78, 8281-8289, 10.1021/ac061249n, 2006.

Daellenbach, K. R., Bozzetti, C., Krepelova, A. K., Canonaco, F., Wolf, R., Zotter, P., Fermo, P., Crippa, M., Slowik, J. G., Sosedova, Y., Zhang, Y., Huang, R. J., Poulain, L., Szidat, S., Baltensperger, U., El Haddad, I., and Prevot, A. S. H.: Characterization and source apportionment of organic aerosol using offline aerosol mass spectrometry, Atmos Meas Tech, 9, 23-39, 10.5194/amt-9-23-2016, 2016.

Daellenbach, K. R., Stefenelli, G., Bozzetti, C., Vlachou, A., Fermo, P., Gonzalez, R., Piazzalunga, A., Colombi, C., Canonaco, F., Hueglin, C., Kasper-Giebl, A., Jaffrezo, J. L., Bianchi, F., Slowik, J. G., Baltensperger, U., El Haddad, I., and Prévôt, A. S. H.: Long-term chemical analysis and organic aerosol source apportionment at 9 sites in Central Europe: Source identification and uncertainty assessment, Atmos. Chem. Phys. Discuss., 2017, 1-36, 10.5194/acp-2017-124, 2017.

Decesari, S., Facchini, M. C., Fuzzi, S., and Tagliavini, E.: Characterization of water-soluble organic compounds in atmospheric aerosol: A new approach, J Geophys Res-Atmos, 105, 1481-1489, Doi 10.1029/1999jd900950, 2000.

Decesari, S., Facchini, M. C., Matta, E., Lettini, F., Mircea, M., Fuzzi, S., Tagliavini, E., and Putaud, J. P.: Chemical features and seasonal variation of fine aerosol water-soluble organic compounds in the Po Valley, Italy, Atmos Environ, 35, 3691-3699, Doi 10.1016/S1352-2310(00)00509-4, 2001.

Du, Z. Y., He, K. B., Cheng, Y., Duan, F. K., Ma, Y. L., Liu, J. M., Zhang, X. L., Zheng, M., and Weber, R.: A yearlong study of water-soluble organic carbon in Beijing I: Sources and its primary vs. secondary nature, Atmos Environ, 92, 514-521, 10.1016/j.atmosenv.2014.04.060, 2014.

Dzepina, K., Arey, J., Marr, L. C., Worsnop, D. R., Salcedo, D., Zhang, Q., Onasch, T. B., Molina, L. T., Molina, M. J., and Jimenez, J. L.: Detection of particle-phase polycyclic aromatic hydrocarbons in Mexico City using an aerosol mass spectrometer, International Journal of Mass Spectrometry, 263, 152-170, https://doi.org/10.1016/j.ijms.2007.01.010, 2007.

Farmer, D. K., Matsunaga, A., Docherty, K. S., Surratt, J. D., Seinfeld, J. H., Ziemann, P. J., and Jimenez, J. L.: Response of an aerosol mass spectrometer to organonitrates and organosulfates and

implications for atmospheric chemistry, P Natl Acad Sci USA, 107, 6670-6675, 10.1073/pnas.0912340107, 2010.

Freney, E., Zhang, Y., Croteau, P., Amodeo, T., Williams, L., Truong, F., Petit, J.-E., Sciare, J., Sarda-Esteve, R., Bonnaire, N., Arumae, T., Aurela, M., Bougiatioti, A., Mihalopoulos, N., Coz, E., Artinano, B., Crenn, V., Elste, T., Heikkinen, L., Poulain, L., Wiedensohler, A., Herrmann, H., Priestman, M., Alastuey, A., Stavroulas, I., Tobler, A., Vasilescu, J., Zanca, N., Canagaratna, M., Carbone, C., Flentje, H., Green, D., Maasikmets, M., Marmureanu, L., Minguillon, M. C., Prevot, A. S. H., Gros, V., Jayne, J., and Favez, O.: The second ACTRIS inter-comparison (2016) for Aerosol Chemical Speciation Monitors (ACSM): Calibration protocols and instrument performance evaluations, Aerosol Sci Tech, 53, 830-842, 10.1080/02786826.2019.1608901, 2019.

Fry, J. L., Kiendler-Scharr, A., Rollins, A. W., Wooldridge, P. J., Brown, S. S., Fuchs, H., Dube, W., Mensah, A., dal Maso, M., Tillmann, R., Dorn, H. P., Brauers, T., and Cohen, R. C.: Organic nitrate and secondary organic aerosol yield from NO3 oxidation of beta-pinene evaluated using a gas-phase kinetics/aerosol partitioning model, Atmos Chem Phys, 9, 1431-1449, 2009.

Fry, J. L., Draper, D. C., Zarzana, K. J., Campuzano-Jost, P., Day, D. A., Jimenez, J. L., Brown, S. S., Cohen, R. C., Kaser, L., Hansel, A., Cappellin, L., Karl, T., Roux, A. H., Turnipseed, A., Cantrell, C., Lefer, B. L., and Grossberg, N.: Observations of gas- and aerosol-phase organic nitrates at BEACHON-RoMBAS 2011, Atmos Chem Phys, 13, 8585-8605, 10.5194/acp-13-8585-2013, 2013.

Ge, X. L., Wexler, A. S., and Clegg, S. L.: Atmospheric amines - Part I. A review, Atmos Environ, 45, 524-546, 10.1016/j.atmosenv.2010.10.012, 2011.

529 Ge, X. L., Zhang, Q., Sun, Y. L., Ruehl, C. R., and Setyan, A.: Effect of aqueous-phase processing
530 on aerosol chemistry and size distributions in Fresno, California, during wintertime, Environ Chem,
531 9, 221-235, 10.1071/EN11168, 2012.

532 Graham, B., Mayol-Bracero, O. L., Guyon, P., Roberts, G. C., Decesari, S., Facchini, M. C., Artaxo,
533 P., Maenhaut, W., Koll, P., and Andreae, M. O.: Water-soluble organic compounds in biomass
534 burning aerosols over Amazonia - 1. Characterization by NMR and GC-MS, J Geophys Res-Atmos,
535 107, doi: 10.1029/2001jd000336, 2002.

536 Heikkinen, L., Äijälä, M., Riva, M., Luoma, K., Dällenbach, K., Aalto, J., Aalto, P., Aliaga, D.,
537 Aurela, M., Keskinen, H., Makkonen, U., Rantala, P., Kulmala, M., Petäjä, T., Worsnop, D., and
538 Ehn, M.: Long-term sub-micrometer aerosol chemical composition in the boreal forest: inter- and
539 intra-annual variability, Atmos. Chem. Phys., 20, 3151–3180, https://doi.org/10.5194/acp-20-
540 3151-2020, 2020.

541 Heringa, M. F., DeCarlo, P. F., Chirico, R., Tritscher, T., Dommen, J., Weingartner, E., Richter,
542 R., Wehrle, G., Prévôt, A. S. H., and Baltensperger, U.: Investigations of primary and secondary
543 particulate matter of different wood combustion appliances with a high-resolution time-of-flight
544 aerosol mass spectrometer, Atmos. Chem. Phys., 11, 5945–5957, https://doi.org/10.5194/acp-11-
545 5945-2011, 2011.

546 Hu, W. W., Hu, M., Yuan, B., Jimenez, J. L., Tang, Q., Peng, J. F., Hu, W., Shao, M., Wang, M.,
547 Zeng, L. M., Wu, Y. S., Gong, Z. H., Huang, X. F., and He, L. Y.: Insights on organic aerosol
548 aging and the influence of coal combustion at a regional receptor site of central eastern China,
549 Atmos Chem Phys, 13, 10095-10112, 10.5194/acp-13-10095-2013, 2013.

Hu, W. W., Hu, M., Hu, W., Jimenez, J. L., Yuan, B., Chen, W. T., Wang, M., Wu, Y. S., Chen, C., Wang, Z. B., Peng, J. F., Zeng, L. M., and Shao, M.: Chemical composition, sources, and aging process of submicron aerosols in Beijing: Contrast between summer and winter, J Geophys Res-Atmos, 121, 1955-1977, 10.1002/2015JD024020, 2016.

Huang, R. J., Zhang, Y. L., Bozzetti, C., Ho, K. F., Cao, J. J., Han, Y. M., Daellenbach, K. R., Slowik, J. G., Platt, S. M., Canonaco, F., Zotter, P., Wolf, R., Pieber, S. M., Bruns, E. A., Crippa, M., Ciarelli, G., Piazzalunga, A., Schwikowski, M., Abbaszade, G., Schnelle-Kreis, J., Zimmermann, R., An, Z. S., Szidat, S., Baltensperger, U., El Haddad, I., and Prevot, A. S. H.: High secondary aerosol contribution to particulate pollution during haze events in China, Nature, 514, 218-222, 10.1038/nature13774, 2014.

Huang, X. F., Yu, J. Z., He, L. Y., and Yuan, Z. B.: Water-soluble organic carbon and oxalate in aerosols at a coastal urban site in China: Size distribution characteristics, sources, and formation mechanisms, J Geophys Res-Atmos, 111, D22212, 10.1029/2006jd007408, 2006.

Jacobson, M. C., Hansson, H. C., Noone, K. J., and Charlson, R. J.: Organic atmospheric aerosols: Review and state of the science, Reviews of Geophysics, 38, 267-294, 10.1029/1998RG000045, 2000.

Jimenez, J. L., Canagaratna, M. R., Donahue, N. M., Prevot, A. S. H., Zhang, Q., Kroll, J. H., DeCarlo, P. F., Allan, J. D., Coe, H., Ng, N. L., Aiken, A. C., Docherty, K. S., Ulbrich, I. M., Grieshop, A. P., Robinson, A. L., Duplissy, J., Smith, J. D., Wilson, K. R., Lanz, V. A., Hueglin, C., Sun, Y. L., Tian, J., Laaksonen, A., Raatikainen, T., Rautiainen, J., Vaattovaara, P., Ehn, M., Kulmala, M., Tomlinson, J. M., Collins, D. R., Cubison, M. J., Dunlea, E. J., Huffman, J. A., Onasch, T. B., Alfarra, M. R., Williams, P. I., Bower, K., Kondo, Y., Schneider, J., Drewnick, F.,

572 Borrmann, S., Weimer, S., Demerjian, K., Salcedo, D., Cottrell, L., Griffin, R., Takami, A.,
573 Miyoshi, T., Hatakeyama, S., Shimono, A., Sun, J. Y., Zhang, Y. M., Dzepina, K., Kimmel, J. R.,
574 Sueper, D., Jayne, J. T., Herndon, S. C., Trimborn, A. M., Williams, L. R., Wood, E. C.,
575 Middlebrook, A. M., Kolb, C. E., Baltensperger, U., and Worsnop, D. R.: Evolution of Organic
576 Aerosols in the Atmosphere, Science, 326, 1525-1529, 10.1126/science.1180353, 2009.

577 Karydis, V. A., Tsimpidi, A. P., Lei, W., Molina, L. T., and Pandis, S. N.: Formation of
578 semivolatile inorganic aerosols in the Mexico City Metropolitan Area during the MILAGRO
579 campaign, Atmos Chem Phys, 11, 13305-13323, 10.5194/acp-11-13305-2011, 2011.

580 Kondo, Y., Miyazaki, Y., Takegawa, N., Miyakawa, T., Weber, R., Jimenez, J., Zhang, Q., and
581 Worsnop, D. R.: Oxygenated and water-soluble organic aerosols in tokyo, J. Geophys. Res., 112,
582 D01203, 10.1029/2006JD007056, 2007.

583 Laskin, A., Smith, J. S., and Laskin, J.: Molecular Characterization of Nitrogen-Containing
584 Organic Compounds in Biomass Burning Aerosols Using High-Resolution Mass Spectrometry,
585 Environmental Science & Technology, 43, 3764-3771, 10.1021/es803456n, 2009.

586 Li, H., Zhang, Q., Zhang, Q., Chen, C., Wang, L., Wei, Z., Zhou, S., Parworth, C., Zheng, B.,
587 Canonaco, F., Prévôt, A. S. H., Chen, P., Zhang, H., Wallington, T. J., and He, K.: Wintertime
588 aerosol chemistry and haze evolution in an extremely polluted city of the North China Plain:
589 significant contribution from coal and biomass combustion, Atmos. Chem. Phys., 17, 4751–4768,
590 https://doi.org/10.5194/acp-17-4751-2017, 2017.

591 Li, H., Cheng, J., Zhang, Q., Zheng, B., Zhang, Y., Zheng, G., and He, K.: Rapid transition in
592 winter aerosol composition in Beijing from 2014 to 2017: response to clean air actions, Atmos.
593 Chem. Phys., 19, 11485–11499, https://doi.org/10.5194/acp-19-11485-2019, 2019.

Liu, S., Tao, S., Liu, W., Liu, Y., Dou, H., Zhao, J., Wang, L., Wang, J., Tian, Z., and Gao, Y.: Atmospheric Polycyclic Aromatic Hydrocarbons in North China: A Winter-Time Study, Environmental Science & Technology, 41, 8256-8261, 10.1021/es0716249, 2007.

Lobert, J. M., Scharffe, D. H., Hao, W. M., and Crutzen, P. J.: Importance of biomass burning in the atmospheric budgets of nitrogen-containing gases, Nature, 346, 552-554, 10.1038/346552a0, 1990.

Luo, Y., Zhou, X., Zhang, J., Xue, L., Chen, T., Zheng, P., Sun, J., Yan, X., Han, G., and Wang, W.: Characteristics of airborne water-soluble organic carbon (WSOC) at a background site of the North China Plain, Atmospheric Research, 231, 104668, https://doi.org/10.1016/j.atmosres.2019.104668, 2020.

Mader, B. T., Yu, J. Z., Xu, J. H., Li, Q. F., Wu, W. S., Flagan, R. C., and Seinfeld, J. H.: Molecular composition of the water-soluble fraction of atmospheric carbonaceous aerosols collected during ACE-Asia, J Geophys Res-Atmos, 109, D06206, 10.1029/2003jd004105, 2004.

May, W. E., Wasik, S. P., and Freeman, D. H.: Determination of the solubility behavior of some polycyclic aromatic hydrocarbons in water, Analytical Chemistry, 50, 997-1000, 10.1021/ac50029a042, 1978.

Miyazaki, Y., Kondo, Y., Shiraiwa, M., Takegawa, N., Miyakawa, T., Han, S., Kita, K., Hu, M., Deng, Z. Q., Zhao, Y., Sugimoto, N., Blake, D. R., and Weber, R. J.: Chemical characterization of water-soluble organic carbon aerosols at a rural site in the Pearl River Delta, China, in the summer of 2006, Journal of Geophysical Research: Atmospheres, 114, 10.1029/2009JD011736, 2009.

Ng, N. L., Canagaratna, M. R., Zhang, Q., Jimenez, J. L., Tian, J., Ulbrich, I. M., Kroll, J. H., Docherty, K. S., Chhabra, P. S., Bahreini, R., Murphy, S. M., Seinfeld, J. H., Hildebrandt, L.,

Donahue, N. M., DeCarlo, P. F., Lanz, V. A., Prevot, A. S. H., Dinar, E., Rudich, Y., and Worsnop, D. R.: Organic aerosol components observed in Northern Hemispheric datasets from Aerosol Mass Spectrometry, Atmos Chem Phys, 10, 4625-4641, 10.5194/acp-10-4625-2010, 2010.

Okuda, T., Naoi, D., Tenmoku, M., Tanaka, S., He, K., Ma, Y., Yang, F., Lei, Y., Jia, Y., and Zhang, D.: Polycyclic aromatic hydrocarbons (PAHs) in the aerosol in Beijing, China, measured by aminopropylsilane chemically-bonded stationary-phase column chromatography and HPLC/fluorescence detection, Chemosphere, 65, 427-435, https://doi.org/10.1016/j.chemosphere.2006.01.064, 2006.

Paatero, P.: The multilinear engine - A table-driven, least squares program for solving multilinear problems, including the n-way parallel factor analysis model, J Comput Graph Stat, 8, 854-888, Doi 10.2307/1390831, 1999.

Parworth, C., Fast, J., Mei, F., Shippert, T., Sivaraman, C., Tilp, A., Watson, T., and Zhang, Q.: Long-term measurements of submicrometer aerosol chemistry at the Southern Great Plains (SGP) using an Aerosol Chemical Speciation Monitor (ACSM), Atmos Environ, 106, 43-55, https://doi.org/10.1016/j.atmosenv.2015.01.060, 2015.

Pathak, R. K., Wang, T., Ho, K. F., and Lee, S. C.: Characteristics of summertime PM2.5 organic and elemental carbon in four major Chinese cities: Implications of high acidity for water-soluble organic carbon (WSOC), Atmos Environ, 45, 318-325, 10.1016/j.atmosenv.2010.10.021, 2011.

Pieber, S. M., El Haddad, I., Slowik, J. G., Canagaratna, M. R., Jayne, J. T., Platt, S. M., Bozzetti, C., Daellenbach, K. R., Fröhlich, R., Vlachou, A., Klein, F., Dommen, J., Miljevic, B., Jiménez, J. L., Worsnop, D. R., Baltensperger, U., and Prévôt, A. S. H.: Inorganic Salt Interference on CO2+

637 in Aerodyne AMS and ACSM Organic Aerosol Composition Studies, Environmental Science &
638 Technology, 50, 10494-10503, 10.1021/acs.est.6b01035, 2016.

639 Primbs, T., Piekarz, A., Wilson, G., Schmedding, D., Higginbotham, C., Field, J., and Simonich,
640 S. M.: Influence of Asian and Western United States Urban Areas and Fires on the Atmospheric
641 Transport of Polycyclic Aromatic Hydrocarbons, Polychlorinated Biphenyls, and Fluorotelomer
642 Alcohols in the Western United States, Environmental Science & Technology, 42, 6385-6391,
643 10.1021/es702160d, 2008.

644 Psichoudaki, M., and Pandis, S. N.: Atmospheric Aerosol Water-Soluble Organic Carbon
645 Measurement: A Theoretical Analysis, Environ Sci Technol, 47, 9791-9798, 10.1021/es402270y,
646 2013.

647 Qiu, Y., Xie, Q., Wang, J., Xu, W., Li, L., Wang, Q., Zhao, J., Chen, Y., Chen, Y., Wu, Y., Du,
648 W., Zhou, W., Lee, J., Zhao, C., Ge, X., Fu, P., Wang, Z., Worsnop, D. R., and Sun, Y.: Vertical
649 Characterization and Source Apportionment of Water-Soluble Organic Aerosol with High-
650 resolution Aerosol Mass Spectrometry in Beijing, China, ACS Earth and Space Chemistry, 3, 273-
651 284, 10.1021/acsearthspacechem.8b00155, 2019.

652 Ravindra, K., Sokhi, R., and Van Grieken, R.: Atmospheric polycyclic aromatic hydrocarbons:
653 Source attribution, emission factors and regulation, Atmos Environ, 42, 2895-2921,
654 https://doi.org/10.1016/j.atmosenv.2007.12.010, 2008.

655 Robinson, A. L., Donahue, N. M., Shrivastava, M. K., Weitkamp, E. A., Sage, A. M., Grieshop,
656 A. P., Lane, T. E., Pierce, J. R., and Pandis, S. N.: Rethinking organic aerosols: Semivolatile
657 emissions and photochemical aging, Science, 315, 1259-1262, 10.1126/science.1133061, 2007.

Romakkaniemi, S., Jaatinen, A., Laaksonen, A., Nenes, A., and Raatikainen, T.: Ammonium nitrate evaporation and nitric acid condensation in DMT CCN counters, Atmos Meas Tech, 7, 1377-1384, 10.5194/amt-7-1377-2014, 2014.

Saxena, P., Hildemann, L. M., Mcmurry, P. H., and Seinfeld, J. H.: Organics Alter Hygroscopic Behavior of Atmospheric Particles, J Geophys Res-Atmos, 100, 18755-18770, Doi 10.1029/95jd01835, 1995.

Saxena, P., and Hildemann, L. M.: Water-soluble organics in atmospheric particles: A critical review of the literature and application of thermodynamics to identify candidate compounds, J Atmos Chem, 24, 57-109, Doi 10.1007/Bf00053823, 1996.

Sciare, J., d'Argouges, O., Sarda-Esteve, R., Gaimoz, C., Dolgorouky, C., Bonnaire, N., Favez, O., Bonsang, B., and Gros, V.: Large contribution of water-insoluble secondary organic aerosols in the region of Paris (France) during wintertime, J Geophys Res-Atmos, 116, D22203, doi: 10.1029/2011jd015756, 2011.

Sullivan, A. P., Weber, R. J., Clements, A. L., Turner, J. R., Bae, M. S., and Schauer, J. J.: A method for on-line measurement of water-soluble organic carbon in ambient aerosol particles: Results from an urban site, Geophys Res Lett, 31, L13105, doi: 10.1029/2004gl019681, 2004.

Sullivan, A. P., Peltier, R. E., Brock, C. A., de Gouw, J. A., Holloway, J. S., Warneke, C., Wollny, A. G., and Weber, R. J.: Airborne measurements of carbonaceous aerosol soluble in water over northeastern United States: Method development and an investigation into water-soluble organic carbon sources, Journal of Geophysical Research: Atmospheres, 111, 10.1029/2006JD007072, 2006.

679 Sun, K., Qu, Y., Wu, Q., Han, T., Gu, J., Zhao, J., Sun, Y., Jiang, Q., Gao, Z., Hu, M., Zhang, Y.,
680 Lu, K., Nordmann, S., Cheng, Y., Hou, L., Ge, H., Furuuchi, M., Hata, M., and Liu, X.: Chemical
681 characteristics of size-resolved aerosols in winter in Beijing, Journal of Environmental Sciences,
682 26, 1641-1650, https://doi.org/10.1016/j.jes.2014.06.004, 2014.

683 Sun, Y. L., Zhang, Q., Anastasio, C., and Sun, J.: Insights into secondary organic aerosol formed
684 via aqueous-phase reactions of phenolic compounds based on high resolution mass spectrometry,
685 Atmos Chem Phys, 10, 4809-4822, 10.5194/acp-10-4809-2010, 2010.

686 Sun, Y. L., Zhang, Q., Zheng, M., Ding, X., Edgerton, E. S., and Wang, X. M.: Characterization
687 and Source Apportionment of Water-Soluble Organic Matter in Atmospheric Fine Particles
688 (PM2.5) with High-Resolution Aerosol Mass Spectrometry and GC-MS, Environ Sci Technol, 45,
689 4854-4861, 10.1021/es200162h, 2011.

690 Sun, Y. L., Zhang, Q., Schwab, J. J., Chen, W.-N., Bae, M.-S., Hung, H.-M., Lin, Y.-C., Ng, N.
691 L., Jayne, J., Massoli, P., Williams, L. R., and Demerjian, K. L.: Characterization of near-highway
692 submicron aerosols in New York City with a high-resolution aerosol mass spectrometer, Atmos.
693 Chem. Phys., 12, 2215–2227, https://doi.org/10.5194/acp-12-2215-2012, 2012.

694 Sun, Y. L., Du, W., Wan, Q. Q., Zhang, Q., Chen, C., Chen, Y., Chen, Z. Y., Fu, P. Q., Wang, Z.
695 F., Gao, Z. Q., and Worsnop, D. R.: Real-Time Characterization of Aerosol Particle Composition
696 above the Urban Canopy in Beijing: Insights into the Interactions between the Atmospheric
697 Boundary Layer and Aerosol Chemistry, Environ Sci Technol, 49, 11340-11347,
698 10.1021/acs.est.5b02373, 2015.

699 Sun, Y. L., Du, W., Fu, P. Q., Wang, Q. Q., Li, J., Ge, X. L., Zhang, Q., Zhu, C. M., Ren, L. J.,
700 Xu, W. Q., Zhao, J., Han, T. T., Worsnop, D. R., and Wang, Z. F.: Primary and secondary aerosols

in Beijing in winter: sources, variations and processes, Atmos Chem Phys, 16, 8309-8329, 10.5194/acp-16-8309-2016, 2016.

Timonen, H., Cubison, M., Aurela, M., Brus, D., Lihavainen, H., Hillamo, R., Canagaratna, M., Nekat, B., Weller, R., Worsnop, D., and Saarikoski, S.: Applications and limitations of constrained high-resolution peak fitting on low resolving power mass spectra from the ToF-ACSM, Atmos Meas Tech, 9, 3263-3281, 10.5194/amt-9-3263-2016, 2016.

Ulbrich, I. M., Canagaratna, M. R., Zhang, Q., Worsnop, D. R., and Jimenez, J. L.: Interpretation of organic components from Positive Matrix Factorization of aerosol mass spectrometric data, Atmos Chem Phys, 9, 2891-2918, 10.5194/acp-9-2891-2009, 2009.

Wang, G. H., Wang, H., Yu, Y. J., Gao, S. X., Feng, J. F., Gao, S. T., and Wang, L. S.: Chemical characterization of water-soluble components of PM10 and PM2.5 atmospheric aerosols in five locations of Nanjing, China, Atmos Environ, 37, 2893-2902, 10.1016/S1352-2310(03)00271-1, 2003.

Xu, J., Shi, J., Zhang, Q., Ge, X., Canonaco, F., Prévôt, A. S. H., Vonwiller, M., Szidat, S., Ge, J., Ma, J., An, Y., Kang, S., and Qin, D.: Wintertime organic and inorganic aerosols in Lanzhou, China: sources, processes, and comparison with the results during summer, Atmos. Chem. Phys., 16, 14937-14957, 10.5194/acp-16-14937-2016, 2016.

Xu, L., Guo, H. Y., Weber, R. J., and Ng, N. L.: Chemical Characterization of Water-Soluble Organic Aerosol in Contrasting Rural and Urban Environments in the Southeastern United States, Environ Sci Technol, 51, 78-88, 10.1021/acs.est.6b05002, 2017.

Xu, W., He, Y., Qiu, Y., Chen, C., Xie, C., Lei, L., Li, Z., Sun, J., Li, J., Fu, P., Wang, Z., Worsnop, D. R., and Sun, Y.: Mass spectral characterization of primary emissions and implications in source

apportionment of organic aerosol, Atmos. Meas. Tech., 13, 3205–3219, https://doi.org/10.5194/amt-13-3205-2020, 2020.

Yao, L., Wang, M.-Y., Wang, X.-K., Liu, Y.-J., Chen, H.-F., Zheng, J., Nie, W., Ding, A.-J., Geng, F.-H., Wang, D.-F., Chen, J.-M., Worsnop, D. R., and Wang, L.: Detection of atmospheric gaseous amines and amides by a high-resolution time-of-flight chemical ionization mass spectrometer with protonated ethanol reagent ions, Atmos. Chem. Phys., 16, 14527–14543, https://doi.org/10.5194/acp-16-14527-2016, 2016.

Ye, Z., Liu, J., Gu, A., Feng, F., Liu, Y., Bi, C., Xu, J., Li, L., Chen, H., Chen, Y., Dai, L., Zhou, Q., and Ge, X.: Chemical characterization of fine particulate matter in Changzhou, China, and source apportionment with offline aerosol mass spectrometry, Atmos. Chem. Phys., 17, 2573-2592, 10.5194/acp-17-2573-2017, 2017.

Yu, L., Smith, J., Laskin, A., Anastasio, C., Laskin, J., and Zhang, Q.: Chemical characterization of SOA formed from aqueous-phase reactions of phenols with the triplet excited state of carbonyl and hydroxyl radical, Atmos. Chem. Phys., 14, 13801–13816, https://doi.org/10.5194/acp-14-13801-2014, 2014.

Yu, L., Smith, J., Laskin, A., George, K. M., Anastasio, C., Laskin, J., Dillner, A. M., and Zhang, Q.: Molecular transformations of phenolic SOA during photochemical aging in the aqueous phase: competition among oligomerization, functionalization, and fragmentation, Atmos. Chem. Phys., 16, 4511–4527, https://doi.org/10.5194/acp-16-4511-2016, 2016.

Zappoli, S., Andracchio, A., Fuzzi, S., Facchini, M. C., Gelencser, A., Kiss, G., Krivacsy, Z., Molnar, A., Meszaros, E., Hansson, H. C., Rosman, K., and Zebuhr, Y.: Inorganic, organic and

744 macromolecular components of fine aerosol in different areas of Europe in relation to their water
745 solubility, Atmos Environ, 33, 2733-2743, Doi 10.1016/S1352-2310(98)00362-8, 1999.

746 Zhang, J. K., Sun, Y., Liu, Z. R., Ji, D. S., Hu, B., Liu, Q., and Wang, Y. S.: Characterization of
747 submicron aerosols during a month of serious pollution in Beijing, 2013, Atmos Chem Phys, 14,
748 2887-2903, 10.5194/acp-14-2887-2014, 2014.

749 Zhang, Q., Anastasio, C., and Jimemez-Cruz, M.: Water-soluble organic nitrogen in atmospheric
750 fine particles (PM2.5) from northern California, J Geophys Res-Atmos, 107,
751 4112,10.1029/2001jd000870, 2002.

752 Zhang, Q., Jimenez, J. L., Worsnop, D. R., and Canagaratna, M.: A case study of urban particle
753 acidity and its influence on secondary organic aerosol, Environ Sci Technol, 41, 3213-3219,
754 10.1021/es061812j, 2007.

755 Zhang, Q., Jimenez, J. L., Canagaratna, M. R., Ulbrich, I. M., Ng, N. L., Worsnop, D. R., and Sun,
756 Y. L.: Understanding atmospheric organic aerosols via factor analysis of aerosol mass
757 spectrometry: a review, Anal Bioanal Chem, 401, 3045-3067, 10.1007/s00216-011-5355-y, 2011.

758 Zhang, X., Liu, J., Parker, E. T., Hayes, P. L., Jimenez, J. L., de Gouw, J. A., Flynn, J. H.,
759 Grossberg, N., Lefer, B. L., and Weber, R. J.: On the gas-particle partitioning of soluble organic
760 aerosol in two urban atmospheres with contrasting emissions: 1. Bulk water-soluble organic carbon,
761 Journal of Geophysical Research: Atmospheres, 117, n/a-n/a, 10.1029/2012jd017908, 2012.

762 Zhang, Y. X., Schauer, J. J., Zhang, Y. H., Zeng, L. M., Wei, Y. J., Liu, Y., and Shao, M.:
763 Characteristics of particulate carbon emissions from real-world Chinese coal combustion, Environ
764 Sci Technol, 42, 5068-5073, 10.1021/es7022576, 2008.

765 Zhou, S., Collier, S., Jaffe, D. A., Briggs, N. L., Hee, J., Sedlacek Iii, A. J., Kleinman, L., Onasch,
766 T. B., and Zhang, Q.: Regional Influence of Wildfires on Aerosol Chemistry in the Western US
767 and Insights into Atmospheric Aging of Biomass Burning Organic Aerosol, Atmos. Chem. Phys.,
768 17, 2477-2493, 10.5194/acp-17-2477-2017, 2017.

769 Zhou, W., Xu, W., Kim, H., Zhang, Q., Fu, P., Worsnop, D., and Sun, Y.: A Review of Aerosol
770 Chemistry in Asia: Insights from Aerosol Mass Spectrometer Measurements, Environmental
771 Science: Processes & Impacts, 10.1039/D0EM00212G, 2020.

772 Zong, Z., Wang, X., Tian, C., Chen, Y., Han, G., Li, J., and Zhang, G.: Source and formation
773 characteristics of water-soluble organic carbon in the anthropogenic-influenced Yellow River
774 Delta, North China, Atmos Environ, 144, 124-132,
775 https://doi.org/10.1016/j.atmosenv.2016.08.078, 2016.

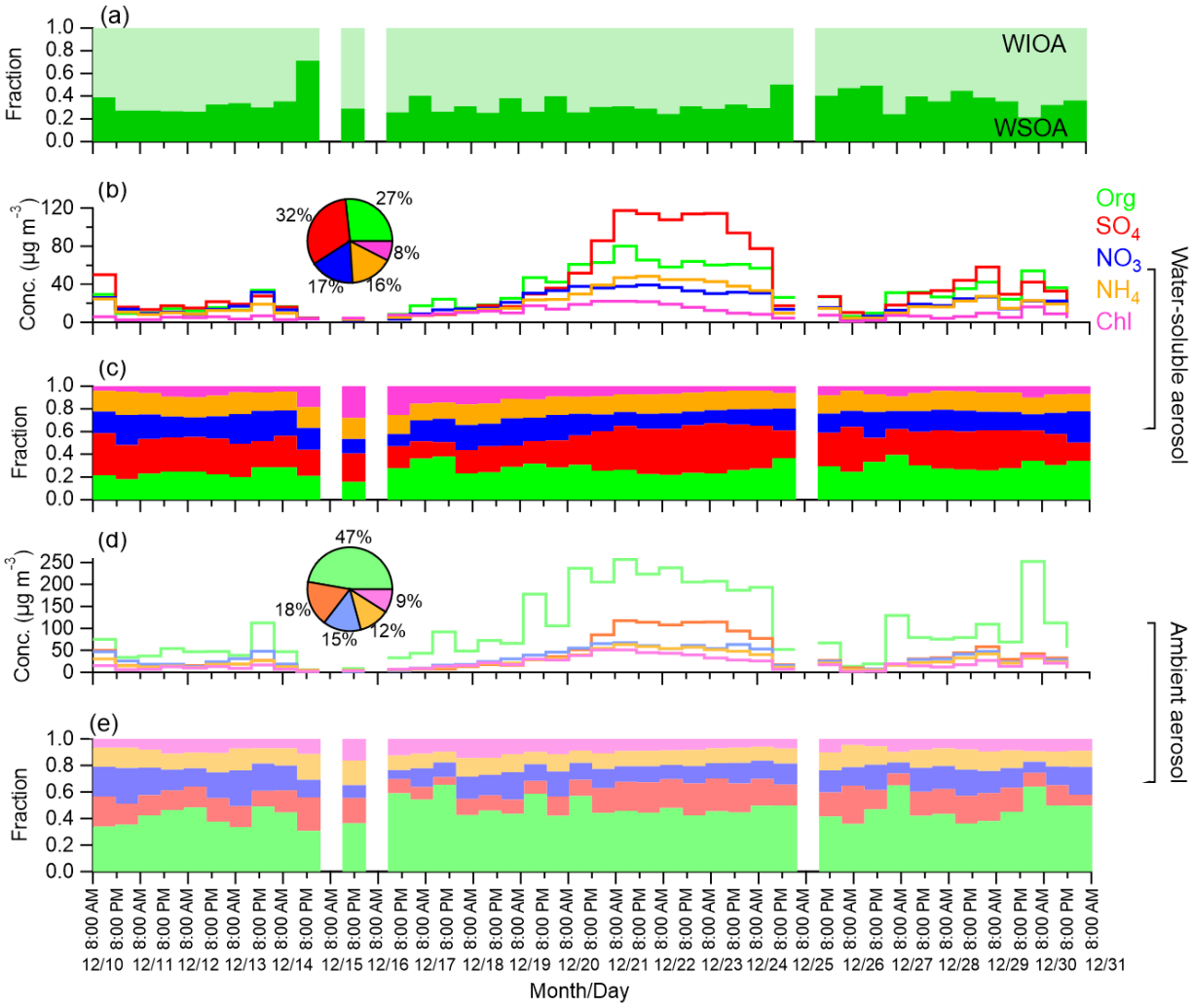

Figure 1. Time series of **(a)** the mass fractional contribution of water-soluble organic aerosol (WSOA) and water-insoluble organic aerosol (WIOA) to total OA, **(b)** the mass concentrations of water-soluble species in $PM_{2.5}$, **(c)** the mass fractional composition of water-soluble $PM_{2.5}$, **(d)** the average ambient mass concentrations of different species during the filter sampling periods, and **(e)** the average mass fractional composition of submicron aerosol during the filter sampling periods.

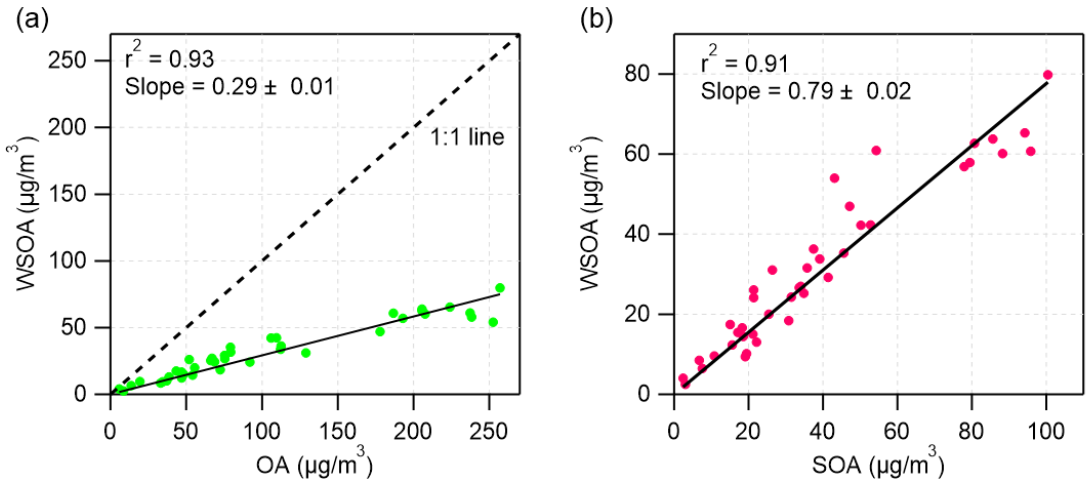

783

784 **Figure 2.** Linear regression correlation between **(a)** WSOA and total OA, and **(b)** WSOA and

785 SOA. The slope is obtained by orthogonal distance regression.

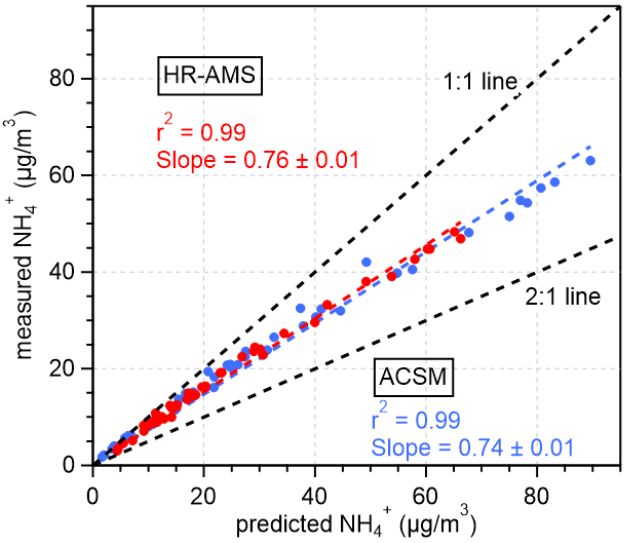

786

787 **Figure 3**. Scatter plots of measured NH_4^+ vs predicted NH_4^+ for water extractions measured by

788 AMS and ambient submicron aerosol measured by ACSM. The predicted NH_4^+ was calculated by

789 assuming full neutralization of the anions - sulfate, nitrate, and chloride.

790

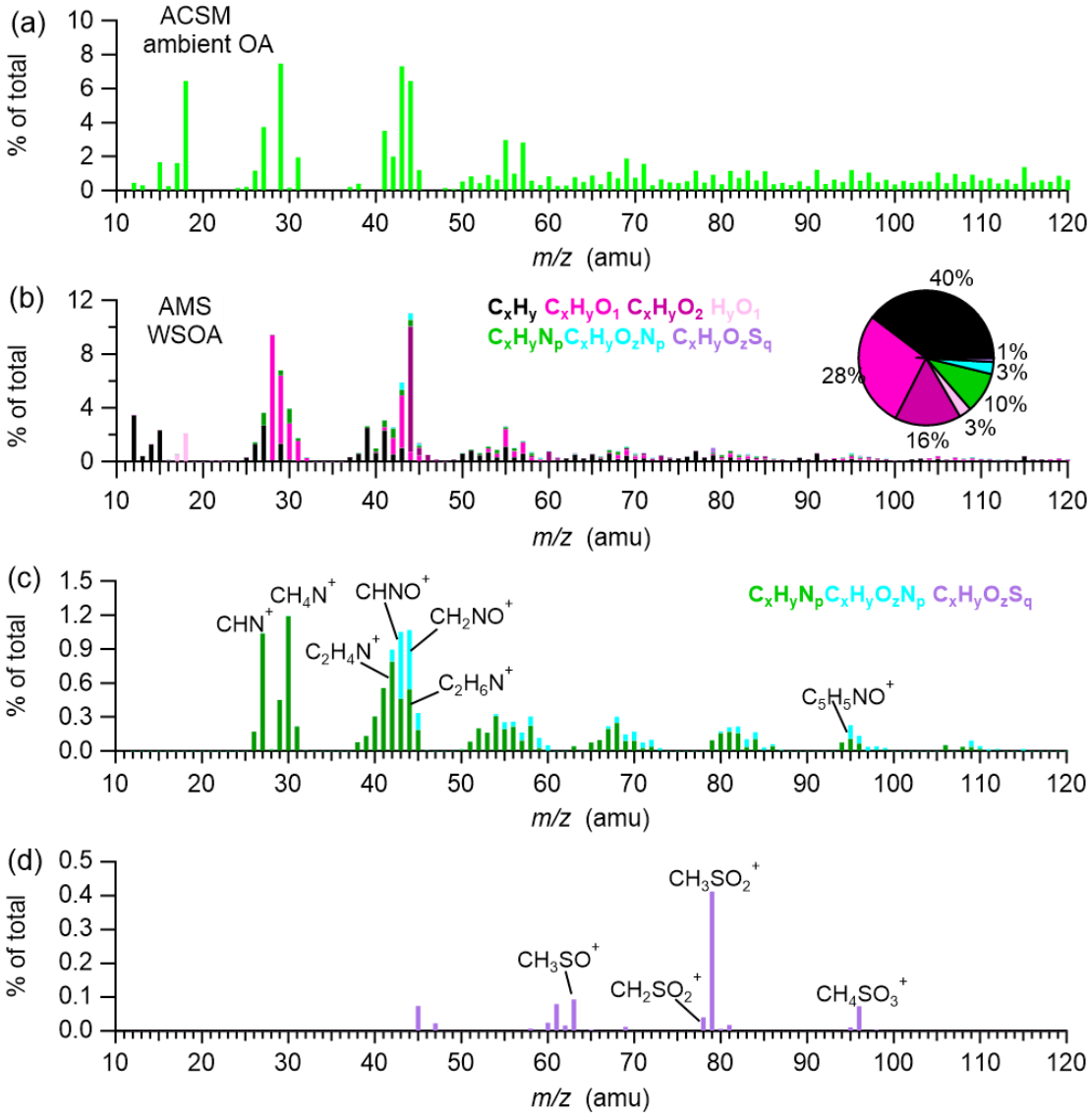

Figure 4. (a) The UMR mass spectra of ambient OA measured by ACSM; **(b)** the average mass spectra of WSOA colored by the contribution of different ion categories; **(c)** the average spectrum of all nitrogen-containing ions of WSOA; **(d)** the average spectrum of all sulfur-containing ions of WSOA.

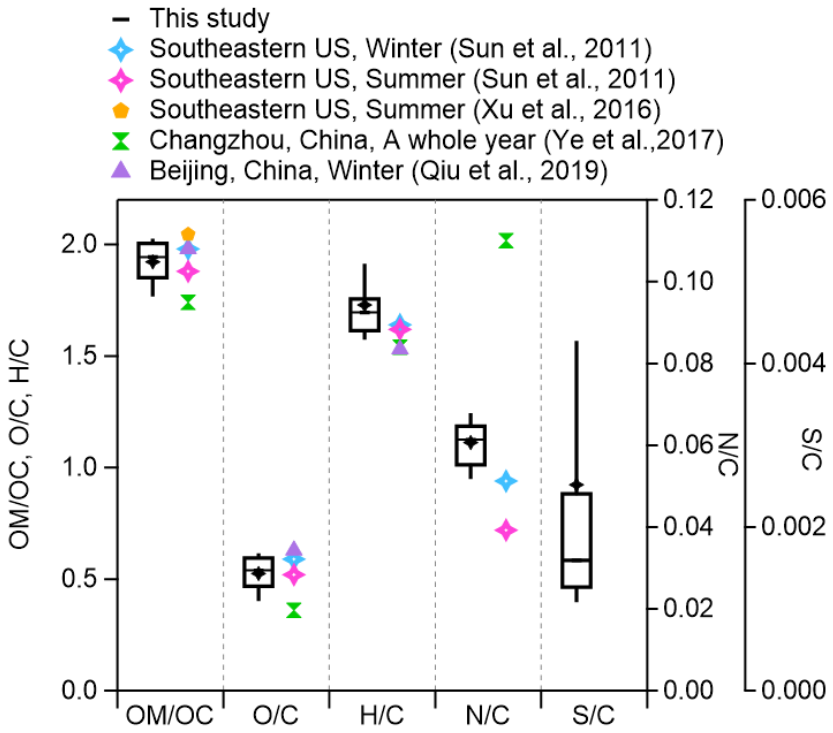

Figure 5. Box and whisker plots of OM/OC, O/C, H/C, N/C, and S/C ratios for WSOA, with the cross representing the mean value, the horizontal line representing the median, the lower and upper of the box representing the 25th and 75th percentiles, and the lower and upper whiskers representing 10th and 90th percentiles. Colored points represent data values from related references for comparison.

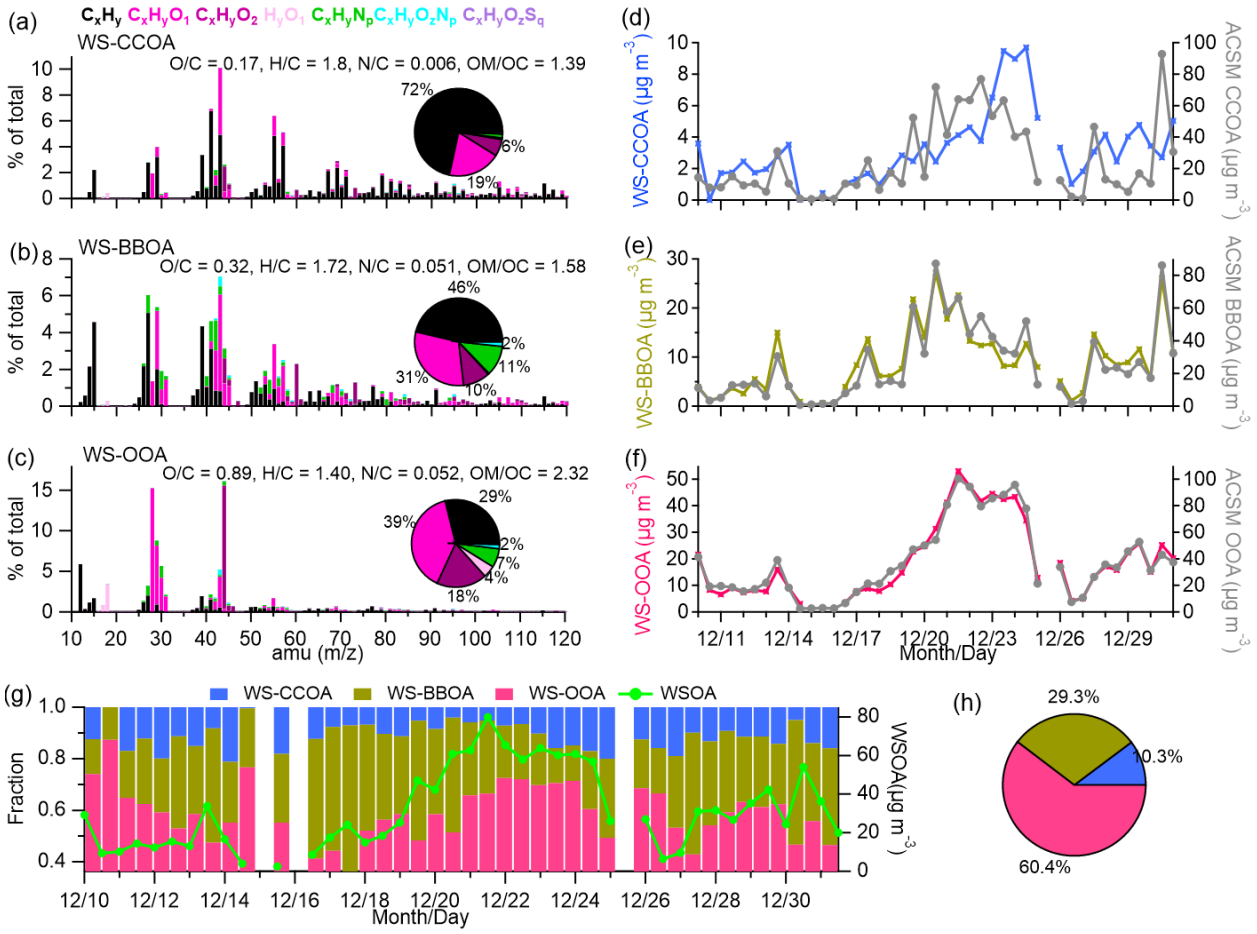

Figure 6. (a-c) HRMS of individual water-soluble OA factors colored by different ion categories; **(d-f)** time series of water-soluble OA factors and the corresponding ambient OA factors; **(g)** time series of the mass fractional composition of WSOA with the total WSOA concentration plotted in green on the right y-axis; **(h)** the average fractional pie chart of WSOA during the study period.

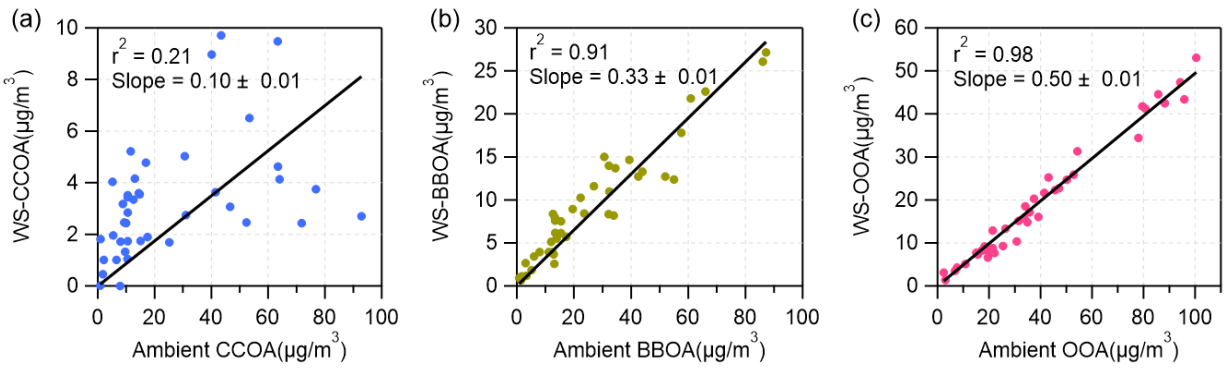

Figure 7. Scatter plots of **(a)** water-soluble CCOA vs. ambient CCOA, **(b)** water-soluble BBOA vs. ambient BBOA, and **(c)** water-soluble OOA vs. ambient OOA. The slope is obtained by orthogonal distance regression.

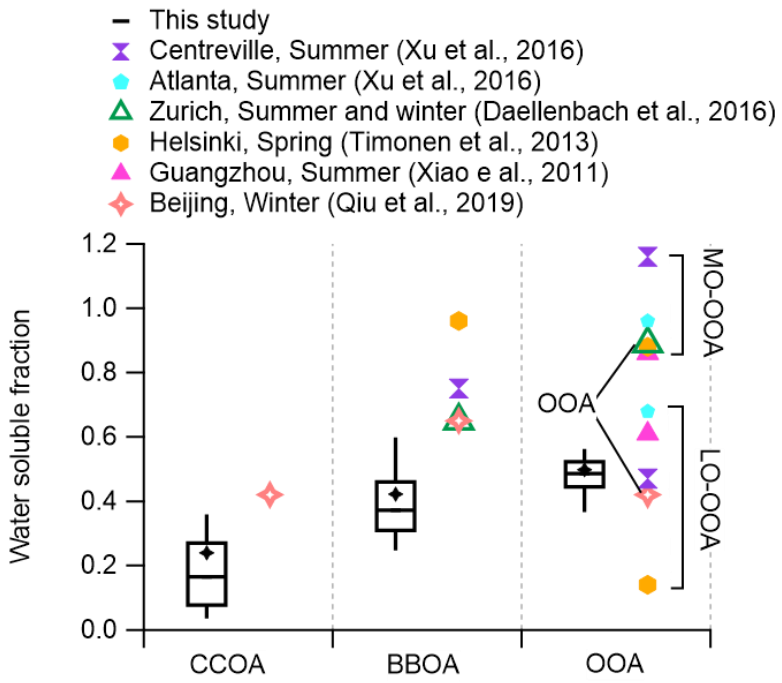

813

814 **Figure 8**. Box and whisker plots of the water-soluble fraction of CCOA, BBOA, and OOA, with
815 the cross representing the mean value, the horizontal line representing the median, the lower and
816 upper of the box representing the 25th and 75th percentiles, and the lower and upper whiskers
817 representing 10th and 90th percentiles. Colored points represent data values from related references
818 for comparison. LO-OOA and MO-OOA refer to the low-oxidized OOA and more-oxidized OOA,
819 respectively.